ELSEVIER

Journal of Volcanology and Geothermal Research 120 (2002) 55–69

Journal of volcanology and geothermal research

www.elsevier.com/locate/jvolgeores

Stratospheric dust loading from early 1981 to September 1985 based on the twilight sounding method and stratospheric dust collections

Nina Mateshvili [a], Frans J.M. Rietmeijer [b,*]

[a] *Abastumani Astrophysical Observatory, Kazbegi av.2a, Tbilisi 380060, Georgia*

[b] *Institute of Meteoritics, Department of Earth and Planetary Sciences, University of New Mexico, Albuquerque, NM 87131-1116, USA*

Received 6 August 2001; accepted 10 April 2002

Abstract

Stratospheric aerosol loading from early 1981 to late 1985 was investigated by remote optical measurements using the twilight sounding method and by in situ mineral dust collections. Both experiments tracked the decay of aerosol abundances after the El Chichón eruption. A comparison between the remote optical observations and dust samplings suggests that aerosol maxima in 1985 were probably associated with a minor eruption of the Bezymianny volcano. Considering the different dynamical behavior of volcanic ash and condensed sulfuric acid aerosol, we traced the origin of collected dust to a minor eruption of Una Una volcano. This collected dust that could not be detected by remote sensing techniques against the high background level due to condensed aerosol from El Chichón highlights the complimentary nature of stratospheric dust collections and the twilight sounding method.

Keywords: stratosphere; aerosol; sulfuric acid; volcanic ash; remote sensing; twilight sounding method; dust collection

1. Introduction

Monitoring the temporal and spatial behavior of stratospheric aerosols following strong volcanic eruptions may contribute to our understanding of the many physical and chemical processes operating in the stratosphere. Stratospheric aerosols may cause shifts of the radiative balance (Dutton and Christy, 1992), affect stratospheric warming (Angell, 1997; Parker and Brownscombe, 1983), possibly contribute to ozone depletion (Hofmann et al., 1993; Chandra, 1993) and cause perturbations in global stratospheric dynamics (Pitari, 1993). Stratospheric aerosols, both condensed aerosols and mineral dusts, might affect global and regional climate changes (Kerr, 1983) during periods of sufficiently rich aerosol injections. Tracking the movements of condensed aerosol, such as sulfuric acid droplets, will offer insights into the complex dynamical processes operating in the stratosphere (Grant et al., 1996).

The stratospheric aerosol and dust were intensively studied following the eruptions of El Chi-

* Corresponding author. Tel.: +1-505-277-5733.
E-mail addresses: matesh@yahoo.com (N. Mateshvili), fransjmr@unm.edu (F.J.M. Rietmeijer).

0377-0273/02/$ – see front matter © 2002 Elsevier Science B.V. All rights reserved.
PII: S0377-0273(02)00360-8

chón (March and April, 1982) using various remote-sensing techniques (Jäger and Hofmann, 1991; Hofmann and Rosen, 1984; Rusch et al., 1994; Eparvier et al., 1994) and in situ dust collections (Gooding et al., 1983; Oberbeck et al., 1983; Mackinnon et al., 1984). In this paper we present two complementary sets of data: (1) stratospheric dust collections during the period from 1981 to September 1985 and (2) optical measurements of the aerosol loading in the stratosphere. We have used the latter previously to monitor abundances and settling of volcanic aerosols after the Mt. St. Helens eruption (Mateshvili et al., 1998), and for meteoritic and meteoric dust in the atmosphere (Mateshvili et al., 1999, 2000). The optical measurements reported here were carried out using the twilight sounding method (TSM) at the Abastumani Observatory during 1983–1985 for altitudes between 20 and 40 km. This technique (Rozenberg, 1966, for a review) continuously traces the stratospheric and mesospheric dust loading as a function of altitude during a twilight period (Link, 1975; Shah, 1970; Ashok et al., 1984). We also used dust data from the NASA Johnson Space Center Cosmic Dust Collection that covered several periods of volcanic quiescence as well as several periods shortly after the El Chichón eruption. We will compare the TSM data with relative abundances of volcanic mineral dust and condensed aerosol obtained by other remote sensing and wire-sampling techniques and integrate the TSM results and the collected, relative mineral dust abundances in the lower stratosphere.

2. Experimental techniques

2.1. The TSM

This technique makes photometric measurements of sky brightness during evening or morning twilight (Fig. 1). When the Sun is within 0–18° below the horizon, the lower part of the atmosphere is in the Earth's shadow while its upper part is sunlit. The boundary between the illuminated and shadowed parts is monotonously shifting up during the evening twilight and down during the morning twilight. The twilight sky brightness at any given moment is caused by the sum of all light that is scattered toward an observer from all air molecules and aerosol particles above this boundary. The lowest, and therefore densest, layer in the sunlit atmosphere at the time of measurement will contribute to the bulk of the scattered light. Light scattering in the atmosphere above the lower sunlit layer can be neglected because of a very rapid decrease of atmospheric density with increasing altitude. Each twilight sky-brightness record contains information on current light-scattering conditions at a height (H) corresponding to the sunlit light-scattering layer described above. A time sequence of such records is converted to a record of variations in the light-scattering ability of the atmosphere as a function of altitude. Excursions in the light-scattering profiles as a function of altitude generally indicate an augmented aerosol loading or a well-defined aerosol layer. A comparative analysis of the twilight curves obtained on consecutive dates reveals temporal variations in atmospheric aerosols from mostly terrestrial sources in the lower stratosphere and from sudden dust intrusions from space, mostly meteor showers, of the mesosphere and upper stratosphere.

The TSM is capable of covering a range of altitudes between 20 and $\sim$140 km. The lower limit is determined by heavy absorption of sunlight passing through the thick lowermost layers of the atmosphere to a scattering air volume and depends on the wavelength used for the observations (Mateshvili et al., 1998). Our single-wavelength measurements were carried out by a photometer equipped with a 610-nm interference filter and using a photomultiplier as a light receiver. At this wavelength the lowest possible detectable altitude is 20 km; using longer wavelengths lowers this limit. The photometer was directed to the point of the solar meridian at zenith distance 60°. Generally, it is possible to estimate the average particle size in an aerosol layer by tracing its settling rate in a time series of individual observations. The average size may be derived from the settling velocity of a dust layer using the Stokes–Davis law. Limitations of the validity of the Stokes–Davis formula and its modifications for

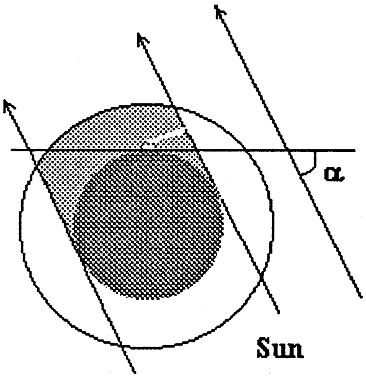

Fig. 1. Schematic diagram showing the conditions during a twilight event. The black disk represents the Earth. Arrows indicate the sunlight's direction; α is a solar depression angle. The outer circle indicates the atmosphere, part of which is sunlit (white) and another part is in the Earth's shadow (gray). The white line indicates light beam scattered to photometer.

some cases of irregular particles are discussed in Fuchs (1964), Reist (1984) and McCartney (1977). Mateshvili et al. (1999, 2000) determined small particles with a 10-nm radius at about 80 km height and large particles (~30-μm radius) between 30 and 50 km height during dust enhancements in the mesosphere associated with known meteor showers. It is not possible to use the TSM procedures to trace the slow settling of an aerosol layer in the lower stratosphere that may be masked by horizontal transport of different layers with a patchy or cloudy structure.

2.2. Stratospheric dust collections

The NASA Johnson Space Center Cosmic Dust Program was initiated in May 1981 for the purpose of collecting extraterrestrial materials that had survived entry into the Earth's atmosphere. Once they settle into the lower stratosphere, they are collected on inertial-impact flat-plate collectors mounted underneath the wings of high-flying aircraft between 17 and 19 km altitude (Mackinnon et al., 1982; Rietmeijer, 1998). Almost all collection flights occur over the Northern Hemisphere with only short tracks south of the equator; they generally follow the eastern Pacific coastline, occasionally up into Alaska. Flights are scheduled to avoid disturbances of the lower stratospheric dust population by ejected volcanic ash and condensed sulfuric acid aerosol because the program's main goal is the collection of extraterrestrial dust. Collections thus occur during volcanically quiescent periods but in 1982 dust was purposely collected in the lower stratosphere for several months following the March–April 1982 eruptions of El Chichón volcano. The individual collection periods were haphazard and the collectors during each period contain the accumulated stratospheric dust from several collection windows that are generally only a few hours long (Rietmeijer and Warren, 1994, for a review). Therefore, normalization of particle abundances to the collector area (cm^2) and collection time (hours), $p/cm^2/h$, is required for comparison of the dust abundances among individual collectors (Rietmeijer and Warren, 1994). Particles are handpicked from the collectors and prepared for preliminary identification using a light-optical microscope (color, size, shape and optical properties) and a scanning electron microscope (image; chemical spectrum). This information is published in the NASA Johnson Space Center Cosmic Dust Catalogs (Rietmeijer and Jenniskens, 2000, for a complete catalog listing). A particle can be identified as (1) cosmic; (2) terrestrial contamination artificial, e.g. spacecraft paint flakes (Zolensky et al., 1989); (3) terrestrial contamination natural (mostly volcanic ash); (4) aluminum oxide sphere (i.e. solid rocket effluents); or (5) 'unknown' (Mackinnon et al., 1982). Handpicking might introduce a bias for certain particle types (e.g. aggregates) or large particles. Several studies showed that collection bias for particles >2 μm is negligible (Zolensky and Mackinnon, 1985; Zolensky et al., 1989; Rietmeijer and Warren, 1994). Any bias is likely to be systematic among the different catalogs. With some caution, the data in the Cosmic Dust Catalogs can be used for comparative purposes of collected dust particles as a function of time (Rietmeijer and Jenniskens, 2000). Error bars on the individual data points will be considerable. It is not considered to be detrimental to the present purpose comparing trends in relative volcanic dust abundances with data obtained by remote-sensing techniques such as TSM.

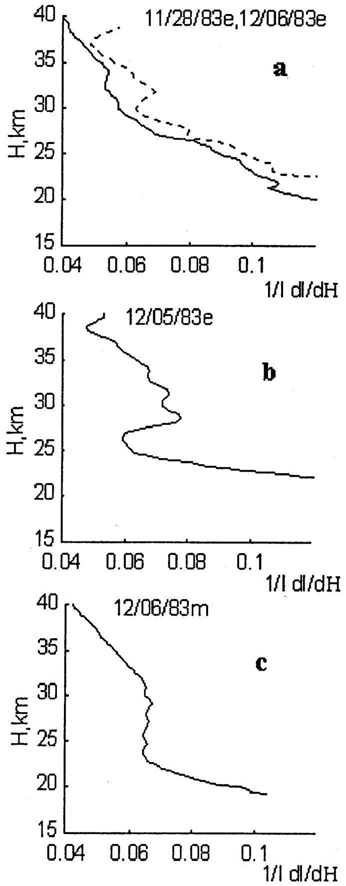

Fig. 2. Normalized derivative of the intensity ($1/I$ dI/dH, in arbitrary units) of the TSM twilight observations as a function of H (km) for 1983 (a) solid line – 11/28/83 evening), dashed line – 12/06/83 evening), (b) 12/05/83, evening, with a prominent maximum at 28 km and (c) 12/06/83, morning.

3. Observations

3.1. TSM data

Measurements of the twilight sky brightness were carried out during three short periods in 1983, 1984 and 1985 (Figs. 2–4) that were characterized by the decay of El Chichón aerosols after a series of eruptions in March and April 1982. We used the normalized derivative ($1/I$ dI/dH; light intensity, I, is in arbitrary units) to emphasize the additional amount of light scattering caused by the dust and condensed aerosols. A typical $1/I$ dI/dH profile shows a general negative slope that is caused by light extinction from light beams passing through the dense lower layers of the atmosphere (see, Fig. 1). This path length, and thus the extinction, increases with the increase of the solar depression angle α and altitude $H(\alpha)$: light extinction increases with height causing a negative slope of a normalized derivative profile. The data showed a dusty stratosphere between late November 1983 through August 1985 and the formation of sporadic aerosol layers or clouds (Figs. 2–4). To provide a context for these light-scattering curves, we show typical profiles for a volcanically quiet period and following a major volcanic eruption into the stratosphere (Fig. 5).

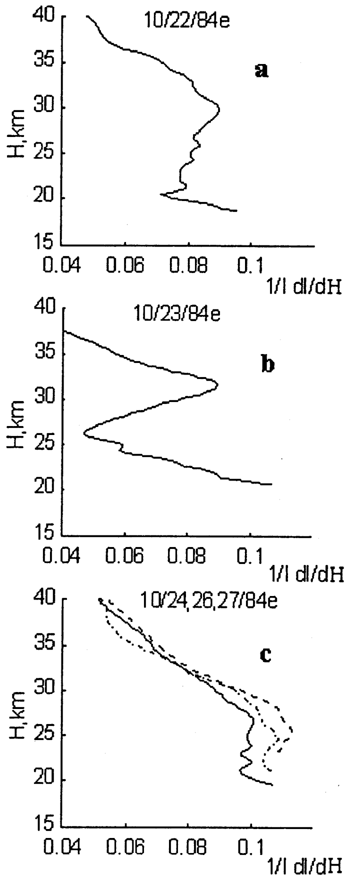

Fig. 3. Same as Fig. 2 for the 1984 TSM observations: (a) 10/22/84 evening, with a maximum at 30 km, (b) 10/23/84 evening and (c) 10/24/84 evening (dash-dotted line), 10/26/84 evening (solid line) and 10/27/84 evening (dashed line).

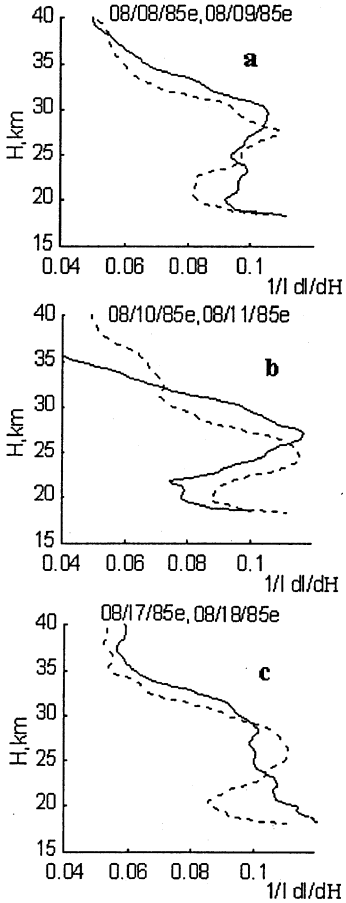

Fig. 4. Same as Fig. 2 for the 1985 TSM twilight observations: (a) solid line – 08/08/85 evening, dashed line – 08/09/85 evening, (b) solid line – 08/10/85 evening, dashed line – 08/11/85 evening, and (c) solid line – 08/17/85 evening, dashed line – 08/18/85 evening.

During late November and early December 1983 (Fig. 2) and again in late October 1984 (Fig. 3), the aerosols between 22 and 35 km altitudes showed substantial variability in the heights of the maximum aerosol concentration at times when a red coloring of the clear twilight sky at the Abastumani Observatory was observed. For example, only vestiges of the strong maximum at 28 km altitude on December 5 (Fig. 2b) remained on the evening of December 6. A rapid clearing of the stratosphere was traced when a maximum at 30 km on October 22 (Fig. 3a) had become a narrow layer at 32 km on October 23 (Fig. 3b). During the next 3 days a more stable layer showing only small variations in shape and amplitude occurred at 25–26 km height (Fig. 3c).

At these times, a stable El Chichón aerosol layer occurred at 18–19 km (Uchino et al., 1985) which is below the lowest possible altitude detectable by TSM. Lidar data showed a pronounced variability in the El Chichón aerosol layer at 28–30 km on a night-to-night basis, and within a given night, between May 1982 and September 1983 (Thomas et al., 1983), particularly during March, August and September, 1983 (Uchino et al., 1985). The evolving TSM layers are consistent with these lidar data.

The data showed a considerable amount of aerosol during August 1985 (Fig. 4) in a well-developed broad layer between 22 and 32 km altitude at a time that the twilight sky had a reddish coloring. This layer with a maximum at 25–28 km displayed minor daily variations. On the evenings of August 9, 10 and 11, it remained stable at approximately the same altitude (Fig. 4a,b). The broader light-scattering profiles for August 17/18 (Fig. 4c) could indicate motion of a non-uniform aerosol layer.

We mention that condensed aerosols and mineral dust from minor volcanic eruptions were present in the stratosphere during the periods of TSM observation. For example, the Bezymianny volcano with a recorded cloud height of 9 km erupted on October 13, 1984 (Bulletin of the Smithsonian Institution, 1984, 1986) just prior to the 1984 TSM observations. Stronger eruptions

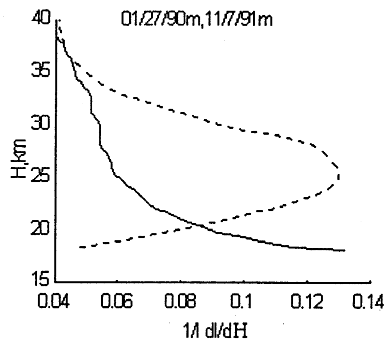

Fig. 5. Same as Fig. 2 showing a typical TSM profile during a volcanically quiescent period (solid line – 01/27/90 morning) and after the 1991 Mt. Pinatubo eruption (dashed line – 11/07/91 morning) obtained at the Abastumani Observatory.

occurred in late June and July 1985 (Bulletin of the Smithsonian Institution, 1986). Satellite observations confirmed penetration of the Una Una 1983 July eruptive cloud into the stratosphere (Bulletin of the Smithsonian Institution, 1983). Minor eruptions will be sources for new additions to the relatively large dust particles from a decaying El Chichón dust population.

3.2. Stratospheric dust

The normalized volcanic ash abundances ($p/cm^2/h$) in three size bins (2–5, 6–10 and >10 μm) from the Cosmic Dust Catalogs are shown in Table 1 along with the time of collection. The complete particle inventories for the collectors U2-9, W7017 and U2024 include abundant particles <1 μm in diameter in the smallest size bin (Zolensky et al., 1989) (Table 1). The data for collector W7017 obtained by Zolensky and Mackinnon (1985) suggest that the 2–5-μm-size bin for all other collectors miss the dominant fraction of volcanic dust <1 μm in diameter. It shows a bias in the catalogs because dust particles <1–2 μm are not handpicked off a collector surface and therefore they are not listed. The maximum dust size or size range on the collector is also listed (Table 1). The collectors contain only small amounts of sulfuric acid droplets. On three collectors the largest grain was a cluster or an aggregate of smaller grains. Large clusters on collector U2001 were undoubtedly from the El Chichón eruptions between March 28 and April 4 when this collector was deactivated in the Cosmic Dust Program because of an extremely high abundance of sulfuric acid droplets.

At this time the collectors were employed to monitor the settling rates for non-spherical particles in the lower stratosphere to compare the observed rates with those calculated by the Wilson–Huang settling law (Mackinnon et al., 1984). Three missions, identified as missions I–III, refer to different collection periods in the lower stratosphere following the El Chichón volcanic eruption (Gooding et al., 1983) (Table 1). The dust was fresh-looking volcanic ash with heavy coatings

Table 1
Normalized ($p/cm^2/h$) particle abundances for volcanic dust in the lower stratosphere (sources: Gooding et al., 1983 and Zolensky et al., 1989)

Source	1–5	2–5	6–10	>10	Max. size	Periods	Remarks
U2-9	1.40	n.a.	0.05	0.02	Unknown	March 1979	Complete inventory
W7013	n.a.	0	0	0.008	59.3	05/22–07/06/81	
W7017	1.55	n.a.	0.102	0.009	Unknown	07/17–09/15/81	Complete inventory
W7017	n.a.	0	0.003	0.008	18.9	07/17–09/15/81	
W7027/29	n.a.	0.0048	0.0038	0.01	27.8	09/15–12/02/81	
U2001	n.a.	0	0.0064	0.008	35.2	03/13–04/08/82	Cluster up to 50 μm
W7039	n.a.	26.68	8.11	3.59	35–40	05/07/1982	Mission I
W7041	n.a.	51.88	9.03	2.67	35–40	07/15/1982	Mission II
W7042	n.a.	8.89	1.56	0.36	35–40	07/16/1982	
W7043	n.a.	5.38	1.02	0.41	35–40	07/16/1982	
W7044	n.a.	68.39	13.49	2.97	35–40	07/20/1982	
W7045	n.a.	1.36	0.25	0.065	30–35	07/21/1982	
W7036	n.a.	6.3	1.75	0.71	20–25	07/29/1982	
W7049	n.a.	9.46	1.13	0.15	20–25	10/13/1982	Mission III
W7055	n.a.	0.62	0.047	0.003	10–15	10/14/1982	
W7054	n.a.	1.52	0.206	0.084	35–40	10/17/1982	
W7050	n.a.	1.34	0.26	0.1	35–40	10/27/1982	
W7052	n.a.	8.7	0.645	0.095	10–15	10/27/1982	
U2015	n.a.	0	0	0.068	33	06/22–08/18/83	Many clusters; largest 150 μm
U2024	10.49	n.a.	0.25	0.16	Unknown	09/30/83–07/13/84	Complete inventory
U2022	n.a.	0	0.0008	0.0056	51.3	04/09–06/26/84	Largest grain is a cluster
U2034	n.a.	0.002	0.008	0.023	33.8	04/17–08/28/85	

n.a.: Not available.

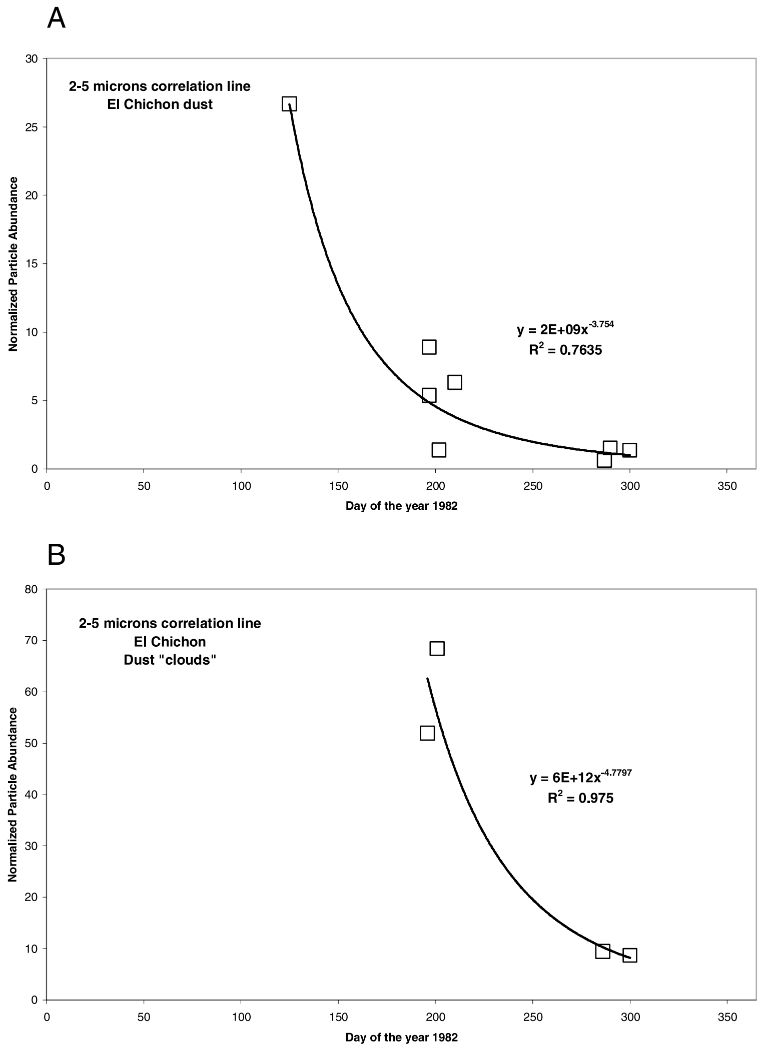

Fig. 6. (a) Normalized (p/cm^2/h) (h; hours) El Chichón dust 2–5 µm in size from missions I–III as a function of time (day of the year) and its (assumed) exponential decay rate. (b) Same for 2–5-µm-sized dust from missions II and III that formed clouds at the time, location and altitude of sampling. Similar plots were obtained for clouds of dust 6–10 µm and $>$10 µm in size (Table 1). This figure and the next two were used to assess dust decay to a background level.

of sulfuric acid droplets and attached sulfate grains (Mackinnon et al., 1984). The results from these missions are shown for dust 2–5 µm in size (Fig. 6a), 6–10 µm (Fig. 7) and $>$10 µm (Fig. 8). Fig. 6b shows the decay of dust 2–5 µm in size that occurred with a higher than average dust abundance during missions II and III. A plausible interpretation is that the lower abundances represent average dust abundances while the higher dust numbers refer to transient dust clouds at the time of sampling. Assuming exponential decay rates, the average El Chichón particle numbers for dust 6–10 µm and $>$10 µm would have decayed to ~0.001 and 0.008 p/cm^2/h, respectively, by mid-1983. At that time, the average (normalized) value for the 2–5-µm-size fraction would be 0.01 p/cm^2/h. The El Chichón 2–5 µm dust fraction would decay to 0.001 p/cm^2/h only after ~5 years (spring 1987). The normalized particle numbers on four post-El Chichón collec-

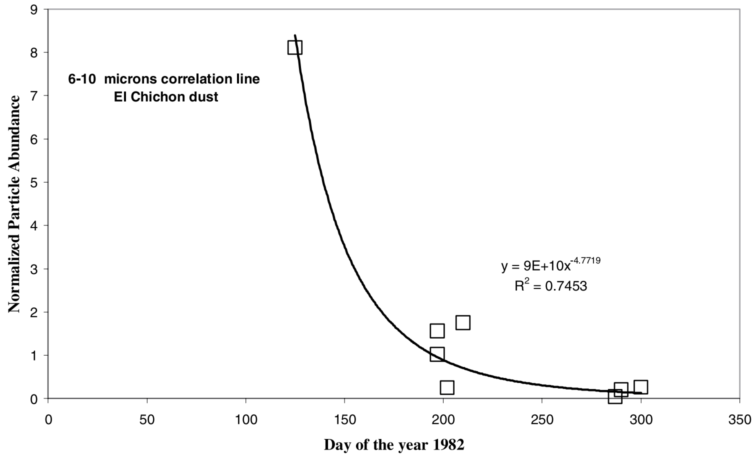

Fig. 7. Normalized (p/cm^2/h) El Chichón dust 6–10 μm in size from missions I–III as a function of time (day of the year) showing an (assumed) exponential day rate.

tors (Table 1) are consistent with the notion that actual decay of its dust was faster.

The collectors listed in Table 1, with the exception of missions I–III, were active during volcanically quiescent periods prior to and following the 1982 El Chichón eruption (Figs. 9–11). The El Chichón dust rapidly decayed to a background of micron-sized volcanic ash that was mostly maintained by periodic ash intrusions from minor volcanic activity. Large, low-density aggregates and small dust particles transported northward in the stratosphere from minor eruptions in the tropics will be a component in this dust background.

4. Discussion

4.1. Condensed or mineral dust aerosol

It is critical to appreciate that TSM measures the integrated light scattered by all particles of different size and composition and cannot distinguish mineral dust from condensed liquid aerosol.

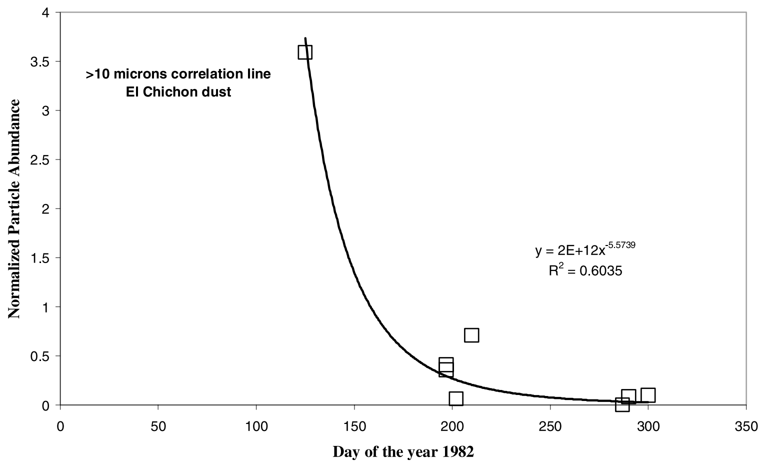

Fig. 8. Normalized (p/cm^2/h) El Chichón dust >10 μm in size from missions I–III as a function of time (day of the year) showing an (assumed) exponential day rate.

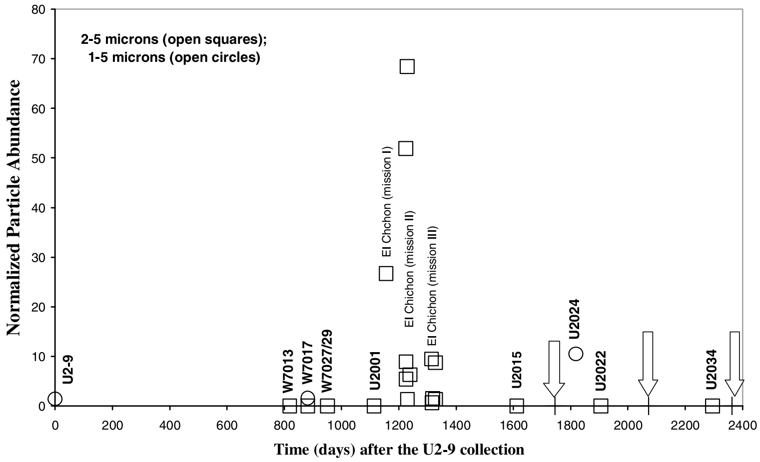

Fig. 9. Normalized 2–5-μm-particle abundances as a function of days after the midpoint date of the collection period of collector U2-9 between March 1979 and September 1985. The times for the collectors are either the midpoint of the collection period or the actual El Chichón sampling date (Table 1) The arrows indicate the times of TSM observation discussed in this paper

Stratospheric aerosols are mostly sulfuric acid droplets with some amount of volcanic ash particles (Russell et al., 1996) but their relative abundances strongly depend on the time after an eruption, eruption type, altitude and latitude and aerosol size. For example, tracking the El Chichón cloud using satellite sensors for a few days after the eruption, Schneider et al. (1999) observed the vertical segregation of the SO_2 and ash clouds due to gravitational processes and different wind directions at different heights. Using airborne wire impactors, Oberbeck et al. (1983) found that the condensed aerosol distribution over Baja California at 18–21 km altitude one month after the El Chichón eruption resembled the pre-eruption distribution but with many silicate particles up to 2.3 μm in radius. We note that this type of collection is biased to favor small particle sizes. That is, Gooding et al. (1983) found that ∼30% of El Chichón dust on May 7, 1982

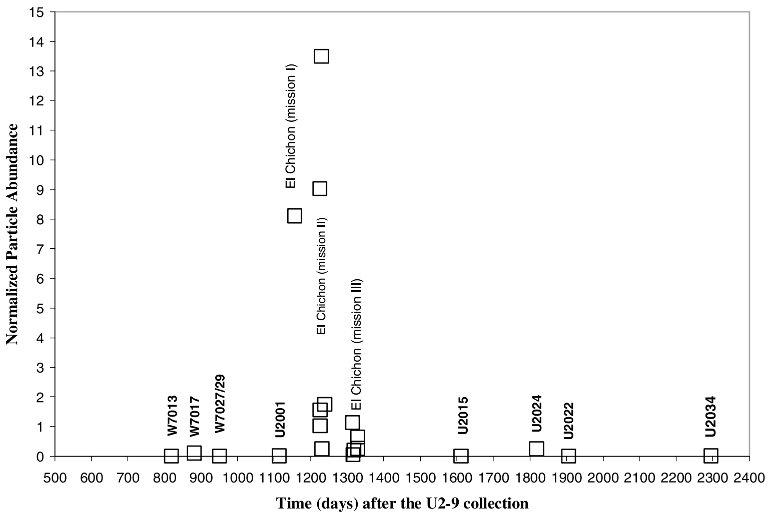

Fig. 10. Normalized 6–10-μm-particle abundances as a function of days after the midpoint date of the collection period of collector U2-9 (Table 1). For collection times see caption of Fig. 9.

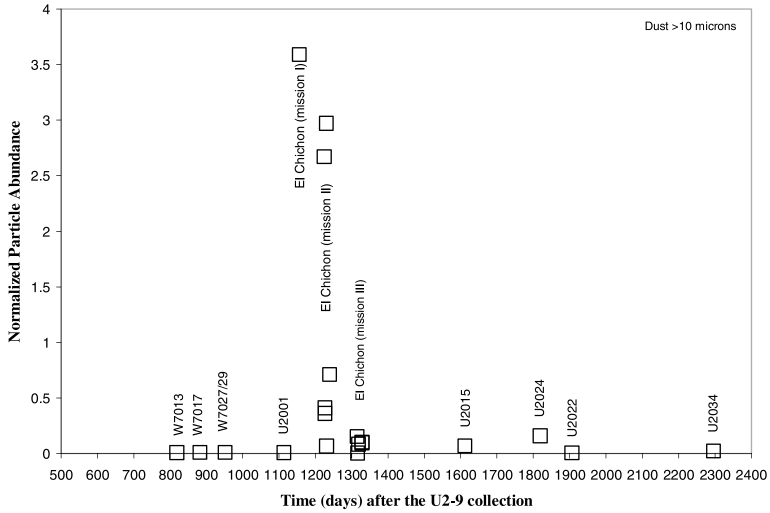

Fig. 11. Normalized >10-μm-particle abundances as a function of days after the midpoint date of the collection period of collector U2-9 (Table 1). For collection times see caption Fig. 9.

was >5 μm in size but their collectors are biased to large (>2 μm) particles. Subsequently, the silicate dust amounts decreased while increasing amounts of condensed aerosols during 1982 November and December had evolved a bimodal distribution with a growing population mode of large sulfuric acid droplets (Oberbeck et al., 1983). In similar experiments during a 9-month period after the Mt. Pinatubo eruption, Pueschel et al. (1994) traced a persistent tri-modal aerosol size distribution, viz. $r_1 = 0.1$ μm, $r_2 = 0.22$ μm, and $r_3 = 0.74$ μm, in the north-polar region at 11 km height. The first and the second modes were sulfuric acid droplets, the third was due to silicate particles coated with sulfuric acid that were occasionally also observed at mid-latitudes. The number of small ($r < 0.2$ μm) sulfuric acid droplets and large volcanic ash particles ($r > 0.6$ μm) increased during the first month after the Mt. Pinatubo eruption (Russell et al., 1996). Over the course of the next 3–6 months the sulfuric acid droplets grew to about 0.5 μm in radius and became the largest detected aerosol particles. From these observations we concluded that large particles with mean radius ~ 1 μm about one month after an eruption are probably mostly volcanic ash; a few months later the predominant aerosols will be mostly large sulfuric acid droplets. Thus, the exact timing of TSM measurements and dust collection flights relative to a major volcanic eruption will critically affect the nature of the detected and collected aerosols. The TSM data cover a period when El Chichón aerosol consisted substantially of evolved sulfuric acid droplets.

4.2. TSM size distribution

The TSM configuration, viz. a 610-nm wavelength and a line-of-sight of 30° above the horizon, will affect the detectable particle size range. The single-wavelength measurements prohibit particle size determination. The intensity of light scattered by aerosol particles of various sizes and composition is strongly wavelength- and viewing-direction-dependent, in particular for relatively large particles showing Mie scattering. Aerosol particle detection by any remote sensing technique based on light scattering depends on wavelength, direction of observations and the aerosol size distribution. The Solar Mesosphere Explorer data for El Chichón stratospheric aerosols (Rusch et al., 1994) illustrate the wavelength dependency. Measurements of the Earth's limb emission were carried out at two wavelengths, 1.27 and 1.87 μm. The 1.27-μm data showed aerosol at 26 km altitude during the period 1982–1987, whereas the

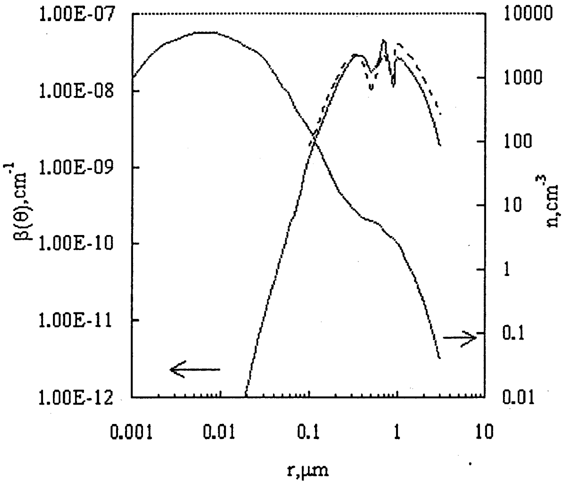

Fig. 12. Measured aerosol distribution 45 days after the El Chichón eruption (Hofmann and Rosen, 1984) (right scale) and appropriate volumetric coefficients of angular scattering, $\beta(\theta)$ (left scale) as a function of the radius of sulfuric acid droplets (solid line) and volcanic ash (dashed line) using the appropriate angular-scattering Mie theory cross-sections.

measurements at 1.87 µm detected aerosol at the same height but only during 1982 and 1983.

The aerosol size distribution at 25 km height ~45 days after the El Chichón eruption (Hofmann and Rosen, 1984) (Fig. 12) coincided with Mission I (Table 1). Since at the time of Mission I volcanic dust abounded in the lower stratosphere, we assumed that large particles in the observed aerosol distribution by Hofmann and Rosen (1984) are volcanic ash. We then calculated the size range for aerosol particles that substantially contributed to the light scattered along the TSM line-of-sight. We could not include ash particles > 3 µm in our calculation because their concentrations can not be estimated from Mission I data. We believe that in most cases their influence is negligible for our purpose because of their high settling rate. Aerosol at 25 km altitude is seen by TSM at $\theta = 33°$ angle, i.e. the sum of the angle between the horizon and line-of-sight (30°) plus the 3° angle of Sun's depression. The calculated volumetric coefficient of angular scattering, $\beta(\theta)$, as a function of particle radius is shown in Fig. 12. We used a wavelength of 610 nm, a refraction coefficient $m = 1.45$ for 75% sulfuric acid droplets and $m = 1.53 - 0.001$ for volcanic ash (Patterson et al., 1983), the particle size distribution in Fig. 12, and the angular-scattering cross-section calculated by Mie theory (Eaton, 1984). The result shows that large particles ($r = 0.2$–2 µm) are clearly the major contributors to the scattered light. Hence, TSM is capable to detect the secondary mode in the particle size distribution reported by Hofmann and Rosen (1984), that, as we have argued, was mostly solid dust for the first month after the El Chichón eruption and was later mainly condensed sulfuric acid aerosol.

Ash particles, $r = 1$ µm, quite effectively scatter light despite their lower concentration compared to smaller particles (Fig. 12). To detect dust particles, their scattered light must exceed the background noise level of Rayleigh scattering by air molecules. The Rayleigh volumetric coefficient of angular scattering, $\beta_1(\theta)$, equals 2.8×10^{-10} cm^{-1} (McCartney, 1977; Penndorf, 1957) at $H = 25$ km and $\theta = 33°$. Even if we assume that the noise level caused by air-density fluctuations is as high as 100% of the magnitude of Rayleigh scattering, the magnitude of the scattered light intensity by aerosols with a size distribution shown in Fig. 12 is still well above the noise level. Thus, TSM detection is optimal at high aerosol concentrations, such as was the case ~45 days after the El Chichón eruption.

The measured sulfuric acid aerosol concentrations show that the period prior to the El Chichón eruption was not volcanically quiescent. It included the eruptions of Mt. St. Helens (1980), Alaid (1981) and Nyamuragira (December 1981/January 1982). The angular-scattering coefficient for the beginning of 1981, the period which was characterized by a low aerosol background, $\beta(\theta) = 2.4 \times 10^{-12}$ cm^{-1}, between 25 and 30 km altitudes was calculated using the modal radius of the aerosol particles (0.2 µm) and aerosol concentrations (0.02 cm^{-3}) from Jäger and Hofmann (1991). This aerosol concentration is well below the TSM detection limit due to Rayleigh scattering. Lidar observations at Mauna Loa showed that aerosol concentrations at the beginning of 1990, i.e. prior to the Kelut eruption, had decreased to the low background level of the beginning of 1981 (Barnes and Hofmann, 1997). The

1990 TSM data showed no maximum during this period (Fig. 5). Using data for the secondary aerosol mode from Jäger and Hofmann (1991), we find $\beta(\theta) = 5 \times 10^{-10}$ cm^{-1} for the period 1983–1985, which is close to the detection limit determined by the noise of Rayleigh scattering. Thus, TSM readily detects minor fluctuations in aerosol concentrations between 25 and 30 km such as sporadic layers. Together with the assumption that the additional light scattering was mainly caused by particles from the secondary mode, we compare the TSM data with the results from other aerosol measurements.

4.3. Analysis of TSM data

Figs. 2–4 show considerable aerosol during the periods of TSM measurements from 1983 to 1985. Lidar data showed overall reduced decay rates of El Chichón aerosol during the fall of 1983 and 1984 (Jäger and Hofmann, 1991). During these periods aerosol transport occurred at 26 km altitude from the tropical stratospheric reservoir to high northern latitudes (Rusch et al., 1994). Similar northward aerosol transport had occurred between 30 and 35 km at the end of 1982 and 1983, while aerosol concentrations in the equatorial region between 26 and 35 km altitude were still high in 1985 (Rusch et al., 1994). The 1983 and 1984 TSM measurements (Figs. 2 and 3) coincided with the periods of northward aerosol transport reported by Rusch et al. (1994). The resulting condensed El Chichón aerosol enhancements caused the transient TSM features detected at mid-latitudes. The prominent and persistent TSM maxima in August 1985 (Fig. 4) are surprising because smaller maxima were expected by comparison with previous years if this aerosol was exclusively associated with El Chichón. Thus, the TSM signal included aerosol from additional sources, most likely a fresh injection of volcanic ash from the Bezymianny eruption in July 1985. The August 1985 TSM signal was mostly caused by coarse-grained, mineral dust with 0.2–2 μm radii rather than evolved sulfuric acid aerosol (Fig. 12), because sulfuric acid droplets could not have grown to this size so quickly after Bezymianny eruption. This is consistent with the higher mineral dust enhancement on collector U2034 flown along the Pacific coast from the Mexican border up to North Alaska between late-April and August 1985 than on U2022 flown during the Spring of 1984 (Table 1). The U2034 collector recorded a sudden but very small dust intrusion. The collectors W7041, W7044, W7049 and W7052 support the formation of ash clouds a few months after the El Chichón eruption. While minor eruptions do not create a uniform, global dust enhancement, they will produce detectable dust clouds.

4.4. Dust collections

These collections are typically solid dust such as volcanic ash rather than condensed aerosol. For example, volcanic silica shards 0.2–2 μm in size with tiny sulfuric acid droplets at their surface were present on the collectors W7027 and W7029 (Table 1) from 1981 May to December with a calculated particle number density of $\sim 10^{-7}$ cm^{-3} (Rietmeijer, 1988). Dust collections are often the only way to detect the effects of minor eruptions against a background of high-condensed-aerosol concentrations from a major eruption.

Hayashida-Amano et al. (1991) reported a relatively unperturbed stratosphere between 10 and 40 km over Tsukuba (Japan) between the eruptions of El Chichón (1982) and the Nevado del Ruiz on November 13, 1985 that reached into the stratosphere. In the months following the Nevado del Ruiz eruption, aerosol layers around 18 km, and up to 26.4 km altitude, had spread northward (Hayashida-Amano et al., 1991). Apparently the stratosphere over Japan was not perturbed by several minor eruptions during this period, e.g. the 1983 July/August Una Una eruption, or aerosol perturbations by minor events were undetectable because of experimental constraints (Hayashida-Amano et al., 1991) or they had not yet arrived. Sulfate aerosol and ash particles from the Gareloi eruption (August 8, 1980) occurred 2 days later over Alaska at 19.2 km altitude that was almost twice as high as the reported plume height at 10.5 km (Sedlacek et al., 1981). Both observations indicate lateral northward and upward migration of stratospheric volcanic aerosols. The use of volatile aerosol tracers has obvious drawbacks. They coagulate, evaporate and re-condense on time scales that cannot always be known (Zhao et al., 1995; Hofmann and Rosen, 1984) and it is difficult to decide whether condensed aerosols indicate transportation or re-condensation processes (Hofmann and Rosen, 1984; Tie et al., 1994). Mineral dust does not suffer from this drawback. It is an inert tracer of stratospheric dynamics.

Different dynamical behavior of mineral dust and condensed aerosol must be considered when comparing collected dust data with optical aerosol measurements. For example, dust abundances had decayed to almost background level within about half a year after the El Chichón eruption (Figs. 6–8) when sulfuric acid aerosol was still abundant relative to the pre-eruption background. Dust is a good tracer of minor eruptions, especially at times of a high-condensed-aerosol background such as in case of the Una Una eruption in July 1983, which occurred a year after El Chichón eruption and thus was difficult to detect optically. The collector U2015 (July to early August 1983) contained extremely large clusters (Table 1). Rietmeijer (1993) suggested that under certain conditions non-spherical particles from minor eruptions located in the tropics could be transported to mid-latitudes. The clusters on this collector are most likely from the Una Una eruption that occurred in tropics in the easterly phase of quasi-biennial oscillation so that its eruption cloud spread along the equator. Considering the easterly wind velocity of 15 m/s at the time of the Una Una eruption (Barnes and Hofmann, 1997), dust from this volcano had reached the US when the collector U2015 was still active. Mackinnon et al. (1984) reported that clusters up to 100 μm in size were still abundant in the lower stratosphere 1 month after the El Chichón eruption. So, clusters similar in size to those collected by U2015 could reach the US from Una Una before gravitational settling had removed them from the collection altitudes. We also suggest that the largest grains on collector U2022 (Table 1) are related to a minor ash intrusion during the 1984 Spring that was probably from the March 16 eruption of Pavlov volcano.

We submitted that the largest grains on a collector during volcanically quiescent periods represent recent injections of volcanic ash from minor eruptions shortly before their collection periods. Collector W7013, that operated from late May to early July 1981, is then of special interest for comparison with the aerosol distributions measured by the SAGE II satellite from July to early August 1981 (Kent and McCormick, 1984: Figs. 4 and 5). The horizontal aerosol distribution had large-scale irregularities, i.e. aerosol was particularly abundant mainly above 16 km altitude near the equator and below 16 km north of 45° latitude with a zone of low aerosol loading that was generally situated over the US (Kent and McCormick, 1984). All 1981-collectors (Table 1) generally followed the Pacific coastline from the equator up to 75°N latitude. At 17–19 km altitudes these collectors traveled from the bottom part of the aerosol cloud near the equator, with abundant large particles as a result of dust settling, into a zone of low aerosol loading over the US. They then continued generally above this cloud at the high latitudes. Thus, we would predict the dearth of small dust particles but presence of large particles on collector W7013 that became active soon after the Pagan eruption (May 15, 1981). This volcano is the most likely source for these large particles than either Alaid (April 27–29, 1981) or Bezymianny (June 16, 1981) that barely intruded the stratosphere following the period of quiescence indicated by collector U2-9 (Table 1). Collector W7013 appears to be free of dust from the May 1980 Mt. St. Helens eruption almost 1 yr earlier. One year is ample time for volcanic ash >2 μm in size from a major eruption to be removed from the lower stratosphere (Figs. 6–8).

We have combined TSM measurements and stratospheric dust collections and find that both techniques are highly complementary to assess the evolution and decay of dust and condensed sulfuric acid aerosol during both volcanically active and volcanically quiescent periods. We stress the qualitative nature of our current effort that can be improved upon by using data sets for atmospheric dynamics and complete particle inventories of collector surfaces down to dust particles <2 μm in size.

5. Summary

We have introduced a new complementary combination of two different sets of data on stratosphere aerosols, viz. (1) remote optical TSM measurements and (2) stratospheric dust collections, that cover a period from early 1981 to September 1985. This period included the 1982 El Chichón eruption and the subsequent decay of its stratospheric aerosol loading. Condensed volcanic aerosols reach maximum concentrations a few months after an eruption. Ash has its maximum immediately following it and decays in a few months. The TSM technique is sensitive to detect coarse-grained condensed aerosol or ash particles such as in 1985 following a minor eruption of the Bezymianny volcano. The comparatively much shorter decay times for solid dust make it possible to detect dust loading and transport from minor eruptions at times of a high condensed-aerosol background from a major eruption. This was the case for dust from the Una Una eruption that occurred one year after the El Chichón eruption.

Acknowledgements

This paper benefited from two critical reviews by an anonymous referee and Mike Zolensky, the NASA/JSC Cosmic Dust Curator. We also would like to express our thanks to Margaret Mangan who handled our paper. We are grateful to Iuri and Giuli Mateshvili for access to the TSM data and for helpful discussions. F.J.M.R. was supported by NASA Grant NAG 5-4441.

References

Angell, J.K., 1997. Stratospheric warming due to Agung, El Chichón, and Pinatubo taking into account the quasi-biennial oscillation. J. Geophys. Res. 102, 9479–9486.

Ashok, N.M., Bhatt, H.C., Chandrasekhar, T., Desai, J.N., Vaidya, D.B., 1984. Twilight optical studies of the El Chichón volcanic dust over Ahmedabad, India. J. Atmos. Terr. Phys. 46, 411–418.

Barnes, J.E., Hofmann, D.J., 1997. Lidar measurements of stratospheric aerosol over Mauna Loa Observatory. Geophys. Res. Lett. 24, 1923–1926.

Bulletin of the Smithsonian Institution, N7, 1983.

Bulletin of the Smithsonian Institution, N10, 1984.

Bulletin of the Smithsonian Institution, N4, 1986.

Chandra, S., 1993. Changes in stratospheric ozone and temperature due to the eruptions of Mt. Pinatubo. Geophys. Res. Lett. 20, 33–36.

Dutton, E.G., Christy, J.R., 1992. Solar radiative forcing at selected locations and evidence for global lower tropospheric cooling following the eruptions of El Chichón and Pinatubo. Geophys. Res. Lett. 19, 2313–2316.

Eaton, N., 1984. Comet dust-applications of Mie scattering. Vistas Astron. 27, 111–129.

Eparvier, F.G., Rusch, D.W., Clancy, R.T., Thomas, G.E., 1994. Solar Mesosphere Explorer satellite measurements of El Chichón stratospheric aerosols. 2: Aerosol mass and size parameters. J. Geophys. Res. 99, 20533–20544.

Fuchs, N.A., 1964. The Mechanics of Aerosol. Pergamon, New York, 351 pp.

Gooding, J.L., Clanton, U.S., Gabel, E.M., Warren, J.L., 1983. El Chichón volcanic ash in the stratosphere: Particle abundances and size distributions after the 1982 eruption. Geophys. Res. Lett. 10, 1033–1036.

Grant, W.B., Browell, E.V., Long, C.S., Stowe, L.L., Grainger, R.G., Lambert, A., 1996. Use of volcanic aerosols to study the tropical stratospheric reservoir. J. Geophys. Res. 101, 3973–3988.

Hayashida-Amano, S., Sasano, Y., Iikura, Y., 1991. Volcanic disturbances in the stratospheric aerosol layer of Tsukuba, Japan, observed by the National Institute for Environmental Studies lidar from 1982 through 1986. J. Geophys. Res. 96, 15469–15478.

Hofmann, D.J., Oltmans, S.J., Harris, J.M., Komhyr, W.D., Lathrop, J.A., Defoor, T., Kuniyuki, D., 1993. Ozone sonde measurements at Hilo, Hawaii following the eruption of Pinatubo. Geophys. Res. Lett. 20, 1555–1558.

Hofmann, D.J., Rosen, J.M., 1984. Balloon-borne particle counter observations of the El Chichón aerosol layers in the 0.01–1.8 μm radius range. Geof. Int. 23-2, 155–185.

Jäger, H., Hofmann, D., 1991. Midlatitude lidar backscatter to mass, area, and extinction conversion model based on in situ aerosol measurements from 1980 to 1987. Appl. Optics 30, 127–138.

Kent, G.S., McCormick, M.P., 1984. SAGE and SAM II measurements of global stratospheric aerosol optical depth and mass loading. J. Geophys. Res. 89, 5303–5314.

Kerr, R.A., 1983. El Chichón climate effect estimated. Science 219, 157.

Link, F., 1975. On the presence of cosmic dust in the upper atmosphere. Planet. Space Sci. 23, 1011–1012.

Mackinnon, I.D.R., McKay, D.S., Nace, G., Isaacs, A.M., 1982. Classification of the Johnson Space Center Stratospheric dust collection. Proc. 13th Lunar Planet. Sci. Conf.. J. Geophys. Res. 87 (Suppl.), A413–A421.

Mackinnon, I.D.R., Gooding, J.L., McKay, D.S., Clanton, U.S., 1984. The El Chichón stratospheric cloud: solid particles and settling rates. J. Volcanol. Geotherm. Res. 23, 125–146.

Mateshvili, I.D., Mateshvili, G.G., Mateshvili, N.I., 1998. Measurement of the vertical aerosol distribution in the middle atmosphere by the twilight sounding method. J. Aerosol Sci. 29, 1189–1198.

Mateshvili, N., Mateshvili, G., Mateshvili, I., Gheondjian, L., Avsajanishvili, O., 1999. Vertical distribution of dust particles in the Earth's atmosphere during the 1998 Leonids. Meteorit. Planet. Sci. 34, 969–973.

Mateshvili, N., Mateshvili, G., Mateshvili, I., Gheondjian, L., Kapanadze, Z., 2000. Dust particles in the atmosphere during the Leonid meteor showers of 1998 and 1999. Earth Moon Planets 82/83, 493–509.

McCartney, E.J., 1977. Optics of the Atmosphere, Scattering by Molecules and Particles. John Wiley, New York, 421 pp.

Oberbeck, V.R., Danielson, E.F., Snetsinger, K.G., Ferry, G.V., Fong, W., Hayes, D.M., 1983. Effect of the eruption of El Chichón on stratospheric aerosol size and composition. Geophys. Res. Lett. 10, 1021–1024.

Parker, D.E., Brownscombe, J.L., 1983. Stratospheric warming following the El Chichón volcanic eruption. Nature 301, 406–408.

Patterson, E.M., Pollard, C.O., Galindo, I., 1983. Optical properties of the ash from El Chichón volcano. Geophys. Res. Lett. 10, 317–320.

Penndorf, R., 1957. Tables of the refractive index for standard air and the Rayleigh scattering coefficient for the spectral region between 0.2 and 20μ and their application to atmospheric optics. J. Opt. Soc. Am. 47, 76–182.

Pitari, G., 1993. A numerical study of the possible perturbation of stratospheric dynamics due to Pinatubo aerosols – Implications for tracer transport. J. Atmos. Sci. 50, 2443–2461.

Pueschel, R.F., Russell, P.B., Allen, D.A., Ferry, G.V., Snetsinger, K.G., 1994. Physical and optical properties of the Pinatubo volcanic aerosol: Aircraft observations with impactors and a Sun-tracking photometer. J. Geophys. Res. 99, 12915–12922.

Reist, P.C., 1984. Introduction to Aerosol Science. Macmillan Publishing Company, New York, 278 pp.

Rietmeijer, F.J.M., 1988. Enhanced residence of small-sized volcanic silica glass and tridymite particles in the lower stratosphere. J. Volcanol. Geotherm. Res. 34, 173–184.

Rietmeijer, F.J.M., 1993. A model for tropical–extratropical transport of volcanic ash in the lower stratosphere. Geophys. Res. Lett. 20, 951–954.

Rietmeijer, F.J.M., 1998. Interplanetary Dust Particles. In: Papike, J.J. (Ed.), Planetary Materials, Rev. Mineral. 36, 2-1–2-95. Mineral. Soc. America, Washington, DC.

Rietmeijer, F.J.M., Jenniskens, P., 2000. Recognizing Leonid meteoroids among the collected stratospheric dust. Earth Moon Planets 82/83, 505–524.

Rietmeijer, F.J.M., Warren, J.L., 1994. Windows of opportunity in the NASA Johnson Space Center Cosmic Dust Collection. In: Zolensky, M.E., Wilson, T.L., Rietmeijer, F.J.M., Flynn, G.J. (Eds.), Analysis of Interplanetary Dust. Am. Inst. Physics Conf. Proc. 310. Am. Inst. Physics Press, New York, pp. 255–275.

Rozenberg, G.V., 1966. Twilight. Plenum Press, New York, pp. 1–380.

Rusch, D.W., Clancy, R.T., Eparvier, F.G., Thomas, G.E., Thomas, R.J., 1994. Solar Mesosphere Explorer satellite measurements of El Chichón stratospheric aerosols. 1: Cloud morphology. J. Geophys. Res. 99, 20525–20532.

Russell, P.B., Livingston, J.M., Pueschel, R.F., Bauman, J.J., Pollack, J.B., Brooks, S.L., Hamill, P., Thomason, L.W., Stowe, L.L., Deshler, T., Dutton, E.G., Bergstrom, R.W., 1996. Global to microscale evolution of the Pinatubo volcanic aerosol derived from diverse measurements and analyses. J. Geophys. Res. 101, 18745–18763.

Sedlacek, W.A., Mroz, E.J., Heiken, G., 1981. Stratospheric sulfate from the Gareloi eruption, 1980: Contribution to the 'ambient' aerosol by a poorly documented volcanic eruption. Geophys. Res. Lett. 8, 761–764.

Shah, G.M., 1970. Study of aerosols in the atmosphere by twilight scattering. Tellus 22, 82–93.

Schneider, D.J., Rose, W.I., Coke, L.R., Bluth, G.J.S., Sprod, I.E., Krueger, A.J., 1999. Early evolution of a stratospheric volcanic eruption cloud as observed with TOMS and AVHRR. J. Geophys. Res. 104, 4037–4050.

Thomas, L., Jenkins, D.B., Wareing, D.P., Farrington, M., 1983. Laser radar observations in mid-Wales of aerosols from the El Chichón eruption. Nature 304, 248–250.

Tie, X., Brasseur, G.P., Briegleb, B., Granier, C., 1994. Two-dimensional simulation of Pinatubo aerosol and its effect on stratospheric ozone. J. Geophys. Res. 99, 20545–20562.

Uchino, O., Tabata, T., Akita, I., Okada, Y., Naito, K., 1985. Ruby lidar observations and trajectory analysis of stratospheric aerosols injected by the volcanic eruptions of El Chichón. Int. Counc. Sci. Unions Handb. MAP 18, 330–336.

Zhao, J., Turco, R.P., Toon, O.B., 1995. A model simulation of Pinatubo volcanic aerosols in the stratosphere. J. Geophys. Res. 100, 7315–7328.

Zolensky, M.E., Mackinnon, I.D.R., 1985. Accurate stratospheric particle size distributions from a flat plate collection surface. J. Geophys. Res. 90, 5801–5808.

Zolensky, M.E., McKay, D.S., Kaczor, L.A., 1989. A tenfold increase in the abundance of large solid particles in the stratosphere, as measured over the period 1976–1984. J. Geophys. Res. 94, 1047–1057.